

See discussions, stats, and author profiles for this publication at: <https://www.researchgate.net/publication/263988081>

# Recovery of Sodium Bicarbonate from Textile Dye Bath Effluent Using Carbon Dioxide Gas

ARTICLE *in* INDUSTRIAL & ENGINEERING CHEMISTRY RESEARCH · NOVEMBER 2013

Impact Factor: 2.59 · DOI: 10.1021/ie402573e

---

READS

25

## 2 AUTHORS:



**Vel Krishnaveni**

Anna University, Chennai

1 PUBLICATION 0 CITATIONS

SEE PROFILE



**Kandasamy Palanivelu**

Anna University, Chennai

106 PUBLICATIONS 2,865 CITATIONS

SEE PROFILE

# Recovery of Sodium Bicarbonate from Textile Dye Bath Effluent Using Carbon Dioxide Gas

V. Krishnaveni and K. Palanivelu\*

Centre for Environmental Studies, Anna University, Chennai 600 025, India

**ABSTRACT:** Water pollution from textile industries is caused by the disposal of brackish dye bath effluent, containing a high concentration of sodium chloride. The targeted removal of  $\text{Na}^+$  from the effluent using carbon dioxide would provide environmental benefits, both in reducing the environmental impact of disposal and in the production of valuable bicarbonate product. This paper describes a method based on the Solvay process for converting  $\text{Na}^+$  in the saline effluent to a useful product. The production of sodium bicarbonate from the effluent using carbon dioxide has been elucidated in a batch mode. The influence of various operating conditions including concentration of ammonium hydroxide, reaction temperature, carbonation time, and the flow rate of carbon dioxide gas on the bicarbonate yield was analyzed. Moreover, the efficiency of struvite precipitation in the removal of  $\text{NH}_4^+$  from the resulting solution of the modified Solvay process was evaluated. The highest  $\text{Na}^+$  removal of 38% of the saline effluent and the best removal efficiency of 80% for  $\text{NH}_4^+$  of the resulting solution were obtained. The results obtained show a feasible way to protect our environment by utilizing the brackish dye bath effluent and the industrial waste gas carbon dioxide in bicarbonate production.

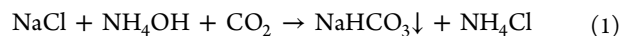
## 1. INTRODUCTION

Carbon dioxide is the most prevalent greenhouse gas that traps heat and raises the global temperature, contributing to climate change. There are various sources of carbon dioxide emissions, which are dominated by combustion of liquid, solid, and gaseous fuels.<sup>1</sup> Carbon dioxide is present in the atmosphere with a volumetric concentration of 0.039%, as of July 2012. There are increasing concerns for global warming and heightened interest worldwide for reducing the emissions of greenhouse gases, particularly carbon dioxide.<sup>2</sup> Existing techniques to sequester carbon dioxide from power plants are forestation, ocean fertilization, mineral carbonation, underground injection, and direct ocean dump.<sup>3</sup> There are ecological concerns, regarding the consequences of storing carbon dioxide in the ocean and in the geological formations as well as the extensive energy required to implement the existing carbon dioxide sequestration techniques.<sup>4</sup> Proper use of carbon dioxide for chemical processing can add value to carbon dioxide gas disposal by making industrially useful carbon-based products. Carbonation is capable of binding a significant amount of carbon dioxide. New technologies and methods, which involve the use of the carbon dioxide in the production of carbonate materials, offer a new route to reduce the carbon dioxide concentration in our atmosphere.<sup>5</sup>

Textile dyeing industries discharge effluent ranging between 100 and 200  $\text{m}^3/\text{t}$  of production.<sup>6</sup> During the reactive dyeing of cotton, salts including sodium chloride (25–80  $\text{kg}/\text{m}^3$ )<sup>7</sup> are placed in a dye bath to aid the exhaustion of various dyes onto the fabric, while bases are added to raise the pH from 7 to 11 to achieve fixation. Afterward, the dye bath spent liquor is discharged with almost all the salt after the removal of color. Consequently, many raw materials are lost in the waste stream ending up in the environment as pollutants. Conventional methods for brine management are disposal via deep well injection, land disposal, evaporation ponds, and mechanical or thermal evaporation.<sup>5</sup> Evaporation ponds are widely used for

brine disposal. Although high temperature and consequently high evaporation rates speedup water reduction, evaporation ponds still suffer from many drawbacks including the need for huge areas and the possibility of contaminant leakage into soil and groundwater.<sup>5</sup> An alternative approach is further processing the effluent to extract all the salts.<sup>8,9</sup> This has the advantages of being environmental friendly and for the production of valuable carbonate chemicals.

The present work evaluates a novel approach that utilizes a chemical reaction based on the Solvay process for converting the industrial waste gas carbon dioxide to a valuable bicarbonate product using textile dye bath effluent. In the process, carbon dioxide is passed into an ammoniated brine solution, which reacts with sodium chloride to form a precipitate of sodium bicarbonate and a soluble ammonium chloride<sup>10</sup> according to the following equation:



The focus of the study was on the recovery/conversion of  $\text{Na}^+$  in the textile dye bath effluent to sodium bicarbonate using carbon dioxide. The process involves the absorption of carbon dioxide in an ammoniated dye bath to give a valuable product, sodium bicarbonate. The process has the dual benefit of decreasing  $\text{Na}^+$  in the textile dye bath effluent and reducing carbon dioxide emissions to the atmosphere through the valuable bicarbonate production.<sup>10</sup> The potential of struvite precipitation on the removal of  $\text{NH}_4^+$  as MAP (magnesium ammonium phosphate hexahydrate;  $\text{MgNH}_4\text{PO}_4 \cdot 6\text{H}_2\text{O}$ ) using  $\text{Mg}^{2+}$  and  $\text{PO}_4^{3-}$  from the resulting solution of the modified Solvay process was also evaluated.

**Received:** August 6, 2013

**Revised:** October 21, 2013

**Accepted:** November 5, 2013

**Published:** November 6, 2013

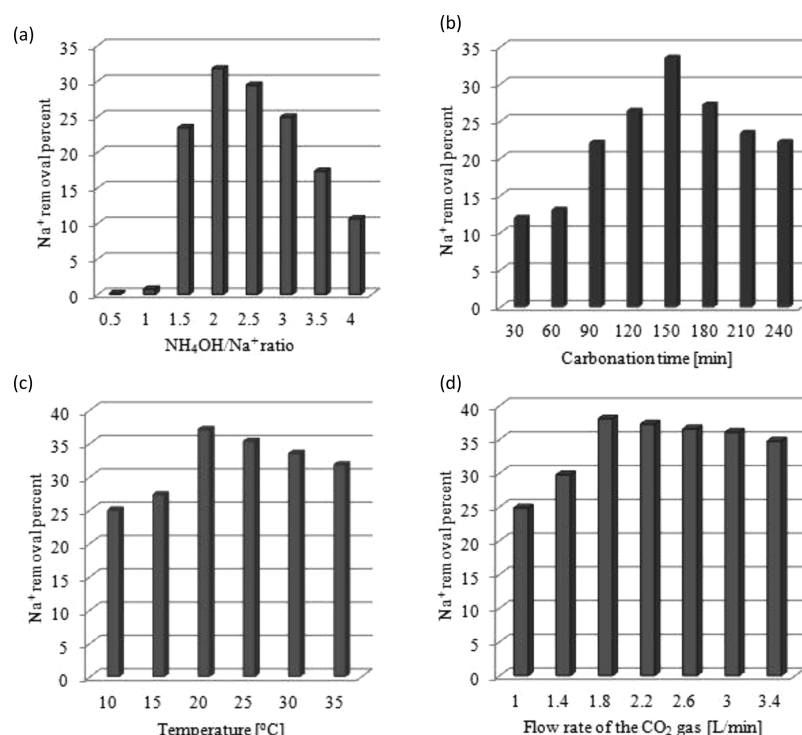


**Figure 1.** Effect of (a)  $\text{NH}_4\text{OH}/\text{Na}^+$  molar ratio (experimental conditions: reaction time, 120 min; reaction temperature, 30 °C;  $\text{CO}_2$  gas flow rate, 2 L/min), (b) carbonation time (experimental conditions:  $\text{NH}_4\text{OH}/\text{Na}^+$  ratio, 2; reaction temperature, 30 °C;  $\text{CO}_2$  gas flow rate, 2 L/min), (c) reaction temperature (experimental conditions:  $\text{NH}_4\text{OH}/\text{Na}^+$  ratio, 2; carbonation time, 150 min;  $\text{CO}_2$  gas flow rate, 2 L/min), and (d) flow rate of  $\text{CO}_2$  gas (experimental conditions:  $\text{NH}_4\text{OH}/\text{Na}^+$  ratio, 2; carbonation time, 150 min; reaction temperature, 20 °C) on  $\text{Na}^+$  removal efficiency.

## 2. MATERIALS AND METHODS

**2.1. Materials.** All chemicals used were of analytical grade. The textile dye bath effluent was collected from the textile dyeing industry situated in Erode, Tamil Nadu, India. Ammonia solution with 25% w/v  $\text{NH}_3$ , purchased from Merck, India, was employed to ammoniate the effluent. Research grade carbon dioxide gas, 99.9%, was purchased from Supreme Engineering Services; India, and used as a source of carbon dioxide. Magnesium chloride hexahydrate and dipotassium hydrogen phosphate were used as received from Merck, India, and fed as a source of  $\text{Mg}^{2+}$  and  $\text{PO}_4^{3-}$ , respectively. Sodium hydroxide purchased from Merck, India, was used to control the pH of the solution. All experimental solutions were prepared using demineralized water.

**2.2. Apparatus and Procedure.** A carbon dioxide gas absorption reactor made of Plexiglas with an inner diameter of 90 mm and an overall height of 170 mm was used in the study, where 500 mL of ammoniated dye bath effluent was exposed to a continuous flow of carbon dioxide gas at a certain flow rate and a fixed time. Carbon dioxide gas was passed through a special feeding tube with a diffuser at the end to generate fine bubbles and endure intense mixing. The tube was extended to the bottom of the reactor tank. The reactor was equipped with several ports for gas and liquid feeds. A peristaltic pump was used to recycle the ammoniated effluent as well as to enhance mixing.

In the struvite precipitation process, 50 mL of the supernatant of the modified Solvay process in a 250 mL of conical flask was mixed with the measured salts of magnesium chloride hexahydrate and dipotassium hydrogen phosphate, and the solution pH was adjusted to 9 by adding sodium hydroxide solution. Mixing was accomplished through a Shaker run at 130

rpm for 3 h, and the supernatant was decanted into a bottle and then analyzed for  $\text{NH}_4^+$  of the supernatant. The sodium bicarbonate and the struvite precipitates were dried at 105 °C for an hour and preserved for further characterization. All the experiments were carried out in duplicate.

**2.3. Analytical Techniques.** At the end of each experiment, the reactor contents were drained from the reactor and filtered. The solids were kept in an oven at 105 °C for a period of 1 h and then used for SEM, XRD, and FTIR analyses. The filtrate was analyzed for  $\text{Na}^+$  in the saline effluent using a flame spectrophotometer (Systronics FPM 128), while the solid was analyzed for the estimation of sodium carbonate and sodium bicarbonate by the alkalinity titration method.<sup>11</sup> The  $\text{NH}_4^+$  was measured by the phenate method<sup>12</sup> using a spectrophotometer (Systronics Visiscan 167). X-ray diffraction patterns were collected using a Philips X'pert MPD system with  $\text{Cu K}\alpha_1$  radiation ( $\lambda = 1.54060 \text{ \AA}$ ) in a  $2\theta$  range of 5–84° at ambient temperature. The SEM images were taken by SEM-JSM 6360 with ion sputter coated with gold target technique. Fourier transform infrared analysis of the precipitate was carried out in a PerkinElmer GX spectrophotometer. The spectra were recorded in the range of 400–4000  $\text{cm}^{-1}$  with a resolution of 4  $\text{cm}^{-1}$  as KBr pellets.

## 3. RESULTS AND DISCUSSION

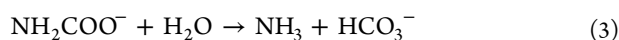
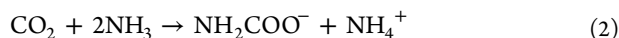
The present study consisted of several batch experiments to determine the efficiency of the modified Solvay process for the removal of  $\text{Na}^+$  from the effluent in the form of sodium bicarbonate using carbon dioxide.

**3.1. Recovery of  $\text{Na}^+$  from Textile Effluent.** **3.1.1. Characterization of Untreated Textile Effluent.** The effluent collected during the study had the following composition

(mg/L): COD, 1588; TDS, 86701;  $\text{Na}^+$ , 27070;  $\text{Cl}^-$ , 41635. The pH and EC of the effluent were 10.6 and 102 mS/cm, respectively. Characteristics of the effluent show a higher concentration of  $\text{Na}^+$  and greater values for TDS, salinity, and COD against allowable limits for the effluent disposal.

**3.1.2. Effect of Concentration of Ammonium Hydroxide on  $\text{Na}^+$  Removal Efficiency.** The role of ammonium hydroxide in the carbonation reaction is important because the ammonium hydroxide buffers the solution at the basic pH.<sup>5</sup> Lack of ammonium hydroxide will obstruct the precipitation of sodium bicarbonate due to the acidic nature of the reactor content.<sup>5</sup> Experiments were conducted with different concentrations of ammonium hydroxide from 1.2 to 9.6 M in the dye bath solution at a reaction temperature of 30 °C and carbon dioxide gas flow rate of 2 L/min for a period of 120 min. The results depicted in Figure 1a indicate that the  $\text{Na}^+$  removal efficiency increased with increasing  $\text{NH}_4\text{OH}/\text{Na}^+$  molar ratio and attained a maximum  $\text{Na}^+$  removal of 31.7% at a  $\text{NH}_4\text{OH}/\text{Na}^+$  ratio of 2. The removal efficiency of  $\text{Na}^+$  was observed to decrease with further increase in the  $\text{NH}_4\text{OH}/\text{Na}^+$  ratio because the excess of ammonium hydroxide reacted with sodium bicarbonate to form an ammonium carbonate. The solubility of sodium chloride was reduced at a higher concentrations of ammonium hydroxide according to a study conducted by Jibril and Ibrahim.<sup>13</sup>

**3.1.3. Effect of Carbonation Time on  $\text{Na}^+$  Removal Efficiency.** Subsequent studies were performed to evaluate the effect of carbonation time on the conversion of  $\text{Na}^+$  in the textile effluent. The carbonation time was varied from 30 to 240 min under identical conditions, that is, reaction temperature of 30 °C,  $\text{NH}_4\text{OH}/\text{Na}^+$  ratio of 2, and the gas flow rate of 2 L/min. The results illustrated in Figure 1b indicate that there was a negligible conversion in the first 30 min and  $\text{Na}^+$  conversion slowly reached the maximum of 33.4% in 150 min. In the early carbonation period, the  $\text{Na}^+$  removal percentage increased due to a higher driving force, resulting from the absorption enhanced reaction between carbon dioxide gas and ammonium hydroxide.<sup>13</sup> However, with further increase in the carbonation time, the  $\text{Na}^+$  conversion efficiency decreased, since the equilibrium of ammonium carbonate approached in the reactions (eqs 2 and 3). Jibril and Ibrahim<sup>13</sup> reported that at the beginning of the conversion, the concentration of ammonium carbonate was predominant, while further carbonation leads to the formation of ammonium bicarbonate followed by sodium bicarbonate, according to the following reactions:



**3.1.4. Effect of Temperature and Flow Rate of Carbon Dioxide Gas on  $\text{Na}^+$  Removal Efficiency.** The carbonation has been investigated at different reaction temperatures from 10 to 35 °C with  $\text{NH}_4\text{OH}/\text{Na}^+$  ratio of 2 and the carbon dioxide gas flow rate of 2 L/min for a period of 150 min. From the results summarized in Figure 1c, it can be seen that the minimum  $\text{Na}^+$  in the filtrate (37% of  $\text{Na}^+$  removal) was observed at the reaction temperature of 20 °C. The increase in carbon dioxide absorption capacity in the ammoniated brine solution is

attributed to the precipitation of sodium bicarbonate. At a higher reaction temperature, the conversion of  $\text{Na}^+$  to sodium bicarbonate was less because the absorption of carbon dioxide gas decreased with the increase in temperature. It was reported that the reaction is exothermic with a negative heat of reaction, up to a temperature of 41 °C.<sup>5</sup> Beyond this temperature, the reaction becomes endothermic.

Subsequent experiments were conducted to test the influence of the gas flow rate on the removal of  $\text{Na}^+$  from the effluent. The flow rate of the carbon dioxide gas was varied between 1 and 3.5 L/min. A plot of  $\text{Na}^+$  removal percentage as a function of the gas flow rate is shown in Figure 1d. The carbon dioxide gas flow rate of 1.8 L/min was found to be the optimum for the maximum  $\text{Na}^+$  removal of 38%. The conversion efficiency of  $\text{Na}^+$  to sodium bicarbonate was increased by increasing the flow rate of carbon dioxide gas, but at a higher flow rate of the gas, the removal of  $\text{Na}^+$  decreased because the diffusivity of the gas decreased with an increase in the flow rate of the gas.<sup>14</sup>

**3.1.5. Characterization of the Carbonate Precipitate.** Precipitation of sodium bicarbonate was carried out under the optimized reaction conditions ( $\text{NH}_4\text{OH}/\text{Na}^+$  ratio of 2, reaction temperature of 20 °C, flow rate of the  $\text{CO}_2$  gas of 1.8 L/min, and the carbonation time of 150 min). The precipitate was dried at 105 °C for an hour and then taken for carbonate and bicarbonate analyses by alkalinity titration method. The 97% sodium bicarbonate and only 3% sodium carbonate were found in the precipitate at the optimized conditions. It is clear that the precipitate formed mainly consists of sodium bicarbonate.

**3.1.5.1. FTIR Analysis.** Much understanding of the molecular structure of a material can be readily obtained through its vibration spectra. The FT-IR spectrum of the solid presented in Figure 2a, matched well with the spectrum found in the literature.<sup>15</sup> The prominent peaks at 1318  $\text{cm}^{-1}$  for sodium

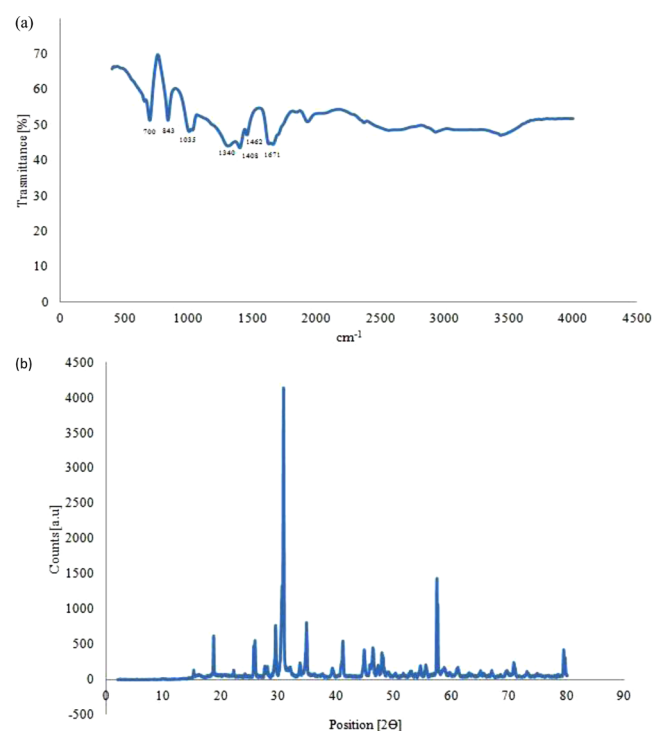


**Figure 2.** (a) FTIR and (b) XRD spectra of the sodium bicarbonate precipitate.



bicarbonate and at  $1405\text{ cm}^{-1}$  for sodium carbonate were due to the carbonate asymmetric stretching. The partial decomposition of the sodium bicarbonate resulted in the formation of sodium carbonate. The FTIR peaks indicate the formation of sodium bicarbonate with negligible amount of sodium carbonate. The band at  $1032\text{ cm}^{-1}$  was assigned to the symmetric stretching mode of the carbonate unit.<sup>16</sup> The IR bands observed at  $1461$  and  $1659\text{ cm}^{-1}$  were assigned to this vibration mode. The occurrence of the peaks at  $842$ ,  $1032$ ,  $1318$ , and  $1659\text{ cm}^{-1}$  suggest the presence of sodium bicarbonate.<sup>17</sup> The combination of peaks at  $1032$ ,  $1318$ , and  $1659\text{ cm}^{-1}$  have been previously assigned to the sodium bicarbonate.<sup>18</sup>

**3.1.5.2. XRD and SEM Analysis.** Sodium bicarbonate was represented by the diffraction lines at  $15.16$ ,  $18.66$ ,  $22.06$ ,  $25.80$ ,  $27.64$ ,  $29.38$ ,  $30.80$ ,  $33.60$ ,  $34.78$ , and  $39.20$  (degree  $2\theta$ ).<sup>17</sup> The XRD pattern (Figure 2b) of the precipitate obtained resembled that of the published result<sup>19</sup> for the sodium bicarbonate. Besides the scanning electron micrograph of the solid (Figure 3) shows a needle type structure similar to the structure of a pure sodium bicarbonate.<sup>5</sup>

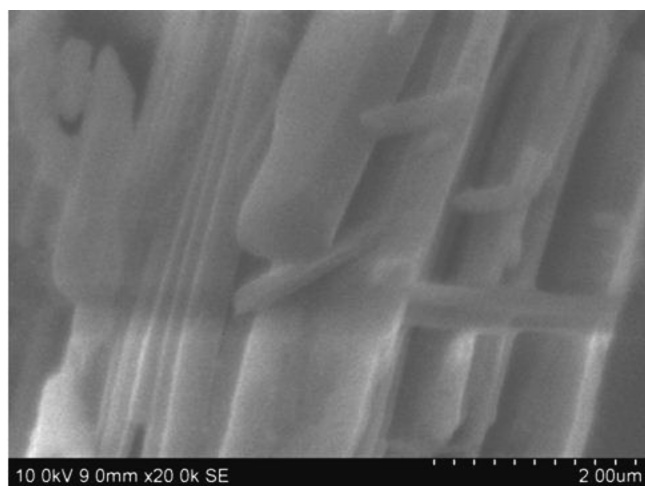


Figure 3. SEM of the sodium bicarbonate precipitate.

**3.1.6. Mass Balance for the Removal of  $\text{Na}^+$ .** Under the optimized conditions, the maximum conversion of sodium chloride from 1 L of dye bath to sodium bicarbonate was  $37.61\text{ g}$  (Figure 4). Following the precipitation of sodium bicarbonate, the resulting solution was taken for  $\text{NH}_4^+$  estimation. This was found to be  $35\text{ g/L}$  in the resulting solution.

**3.2. Recovery of  $\text{NH}_4^+$  from the Supernatant of Modified Solvay Process.** The regeneration of  $\text{NH}_4^+$  from the resulting solution of the Solvay process using activated carbon has been studied.<sup>4</sup> Since this method has a very low  $\text{NH}_4^+$  removal efficiency, an attempt was made to remove  $\text{NH}_4^+$  from the resulting solution of the modified Solvay process as struvite, which is a valuable fertilizer.<sup>20</sup> Subsequent experiments have been undertaken to evaluate the importance of pH and the concentration of  $\text{Mg}^{2+}$  and  $\text{PO}_4^{3-}$  on the removal of  $\text{NH}_4^+$  through MAP precipitation:

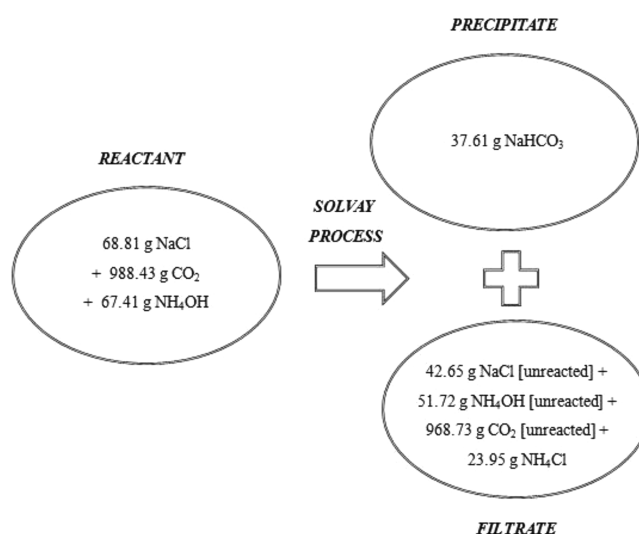
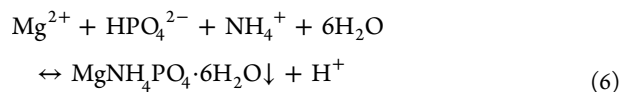
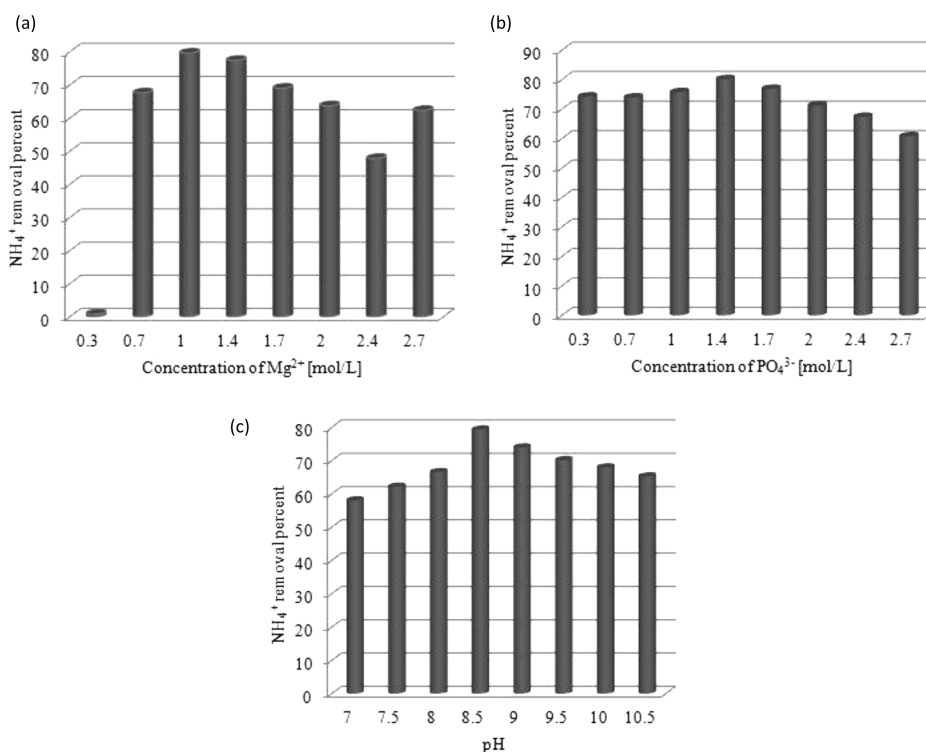


Figure 4. Flowchart of mass balance for the removal of  $\text{Na}^+$  from the dye bath effluent.

**3.2.1. Effect of Concentration of  $\text{Mg}^{2+}$  on  $\text{NH}_4^+$  Removal Efficiency.** Studies were performed to evaluate the effect of  $\text{Mg}^{2+}$  concentration on the removal of  $\text{NH}_4^+$  through MAP precipitation. The concentration of  $\text{Mg}^{2+}$  was varied between  $0.3$  and  $2.7\text{ M}$ , keeping the other conditions (reaction temperature of  $30\text{ }^\circ\text{C}$ ,  $\text{PO}_4^{3-}$  of  $1.7\text{ M}$ , stirring speed of  $130\text{ rpm}$ , and the solution pH of  $9$ ) constant. Figure 5a illustrates that there was an insignificant  $\text{NH}_4^+$  removal of  $2.5\%$  at  $0.3\text{ M}$  and the highest removal of  $80\%$  for  $\text{NH}_4^+$  was obtained at  $1\text{ M}$  of  $\text{Mg}^{2+}$ . A further increase in the concentration of  $\text{Mg}^{2+}$  between  $1.4$  and  $2.7\text{ M}$  caused a slow decrease in the removal efficiency of  $\text{NH}_4^+$ . The removal efficiency of  $\text{NH}_4^+$  decreased in a higher concentration of  $\text{Mg}^{2+}$  because of the coprecipitation of newberyite and cattite in the struvite precipitation.<sup>21</sup> Mijangos et al.<sup>22</sup> have found that at a higher  $\text{Mg}^{2+}$  concentration, the number of magnesium species coprecipitated including magnesium phosphate, reduced the driving force for the precipitation of struvite. The increase of  $\text{Mg}^{2+}$  concentration in the resulting solution accompanied by an increase of the chloride concentration (counterion), resulted in a higher ionic strength and a lower supersaturation ratio with respect to struvite in the solution.<sup>21</sup> They further noted that an increase in the  $\text{Mg}^{2+}$  concentration in the solution not only affected the struvite precipitation but also had a significant effect on the crystal size of the crystalline precipitate.<sup>23</sup> In the latter experiments,  $1\text{ M}$   $\text{Mg}^{2+}$  and reaction time of  $3\text{ h}$  were adopted to obtain high removal efficiency of the  $\text{NH}_4^+$ .

**3.2.2. Effect of Concentration of  $\text{PO}_4^{3-}$  on  $\text{NH}_4^+$  Removal Efficiency.** Experiments were carried out varying the concentration of  $\text{PO}_4^{3-}$ , ranging between  $0.3$  and  $2.7\text{ M}$ , at  $1\text{ M}$   $\text{Mg}^{2+}$  and solution pH of  $9$ . The results depicted in Figure 5b point out that the  $\text{NH}_4^+$  removal percentage increased with increasing the concentration of  $\text{PO}_4^{3-}$  from  $0.3$  to  $1\text{ M}$  and reached the maximum removal of  $80.2\%$  at  $1.4\text{ M}$  of the  $\text{PO}_4^{3-}$ . The conversion efficiency of  $\text{NH}_4^+$  decreased with increasing the  $\text{PO}_4^{3-}$  concentration of  $1.7$  to  $2.7\text{ M}$ , due to the formation of other complexes including magnesium phosphate. The change of  $\text{PO}_4^{3-}$  concentration in the solution was in accordance with the change in pH. Stratful et al.<sup>24</sup> demonstrated that at a higher  $\text{PO}_4^{3-}$  concentration, more hydrogen was released into the solution when struvite is formed, resulting in a decrease in the

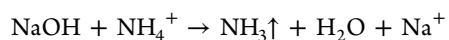


**Figure 5.** Effect of (a) concentration of  $\text{Mg}^{2+}$  (experimental conditions: reaction temperature, 30 °C; concentration of  $\text{PO}_4^{3-}$ , 1.7 M; stirring speed, 130 rpm; pH 9), (b) concentration of  $\text{PO}_4^{3-}$  (experimental conditions: reaction temperature, 30 °C; concentration of  $\text{Mg}^{2+}$ , 1 M; stirring speed, 130 rpm; pH 9), and (c) pH (experimental conditions: reaction temperature, 30 °C; concentration of  $\text{Mg}^{2+}$ , 1 M; stirring speed, 130 rpm; concentration of  $\text{PO}_4^{3-}$ , 1.4 M) on the removal of  $\text{NH}_4^+$ .

pH of the solution. It was therefore speculated that at low pH, further crystallization and precipitation of struvite was inhibited by the dissolution of struvite. This also caused an increase in the residual concentration of  $\text{PO}_4^{3-}$ . Moreover, at a higher concentration of  $\text{PO}_4^{3-}$ , the main product was magnesium dihydrogen phosphate, which leads to an undesired consumption of ions involved in the struvite precipitation.<sup>24</sup>

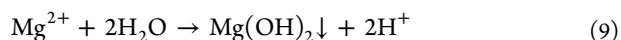
**3.2.3. Effect of pH on  $\text{NH}_4^+$  Removal Efficiency.** The pH is the most important and determining variable in the struvite precipitation. In order to remove struvite from the supernatant by precipitation, the pH value of the solution should be in the pH range of 8.0–9.0, where struvite solubility is minimal. In this study, to determine the optimum pH for the maximum  $\text{NH}_4^+$  removal, experiments were performed with varying pH between 7 and 10.5 with an optimized concentration of 1 and 1.4 M  $\text{Mg}^{2+}$  and  $\text{PO}_4^{3-}$ , respectively. The experimental results are shown in Figure 5c. The  $\text{NH}_4^+$  removal efficiency increased rapidly with the increase in the pH and reached 80% at a pH of 8.5. In the struvite precipitation, the pH of the supernatant decreased at the beginning, which might correspond to the formation of struvite followed by the liberation of  $\text{H}^+$  ions in the supernatant caused by the addition of  $\text{K}_2\text{HPO}_4$  in the pH range of 7–9. The addition of NaOH neutralized the  $\text{H}^+$  ions in the supernatant to control the pH in the range of 8–9 to minimize the struvite solubility and loss of ammonia. The struvite precipitation rate increased with a rise in pH because an increased pH would increase the rate constant by improving the nucleation rate. The improved nucleation would have given more surface area on which crystal growth could take place. When the pH was beyond the optimum range, magnesium phosphate was formed instead of struvite in the process, leading to a decrease in the removal efficiency of  $\text{NH}_4^+$ . Finally, this

resulted in a decrease in the  $\text{NH}_4^+$  removal efficiency.<sup>25</sup> Moreover, if the pH value becomes too high, the  $\text{NH}_4^+$  is converted to ammonia,<sup>26</sup> which would also lower the yield of struvite. The liberation of  $\text{NH}_3$  occurred at a high pH around 10–12 because of the reaction between NaOH and  $\text{NH}_4^+$ .  $\text{NH}_4^+$  removal at above pH 9 might be due to the conversion of  $\text{NH}_4^+$  to  $\text{NH}_3$  at these pH ranges rather than struvite formation.



$$\text{p}K_a = 9.26 \quad (7)$$

If the pH value were slightly alkaline, then the struvite would be the major product. However, with further increase in pH, the product would include magnesium phosphate and magnesium hydroxide and the solubility of struvite would be increased. When the solution pH rises above 10, the following reactions take place easily:



So, the pH not only controls the struvite solubility but also the major removal pathway of  $\text{NH}_4^+$ .

**3.2.4. Struvite Characterization.** **3.2.4.1. XRD and SEM Analysis.** The XRD analysis was used to characterize the purity of the struvite deposits collected from the resulting solution. The X-ray diffractogram exhibited several peaks, indicating the presence of struvite, as illustrated in Figure 6a. The XRD pattern generated from the precipitated matter matched well with the database model for struvite, that is, position and intensity of the peaks.<sup>27</sup> To determine the morphology, the precipitated matter was also examined by SEM and the SEM

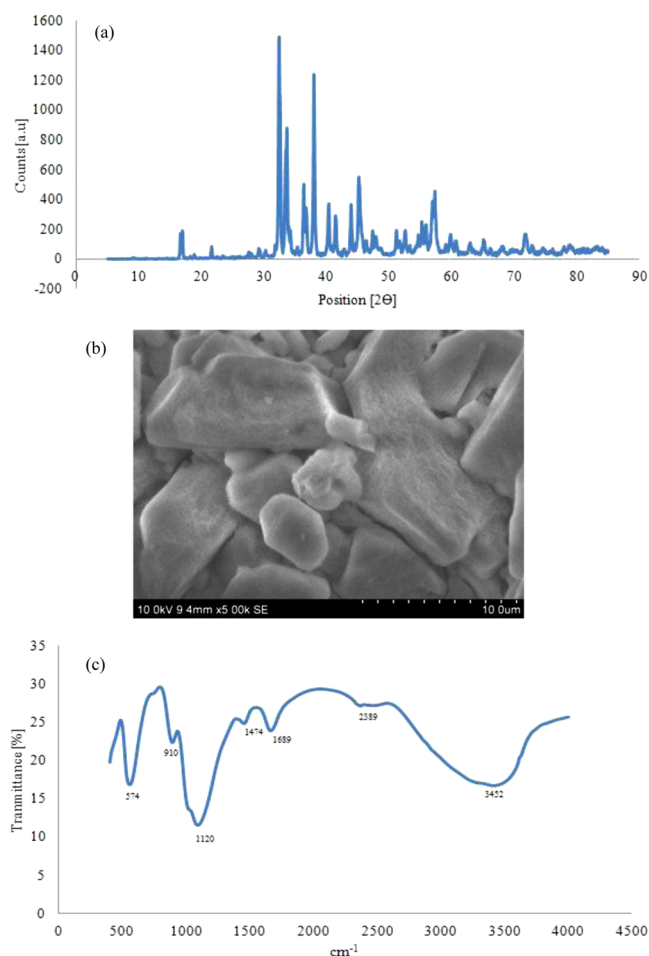


Figure 6. (a) XRD, (b) SEM, and (c) FTIR of the struvite precipitate.

micrograph is illustrated in Figure 6b. Since the crystalline struvite powder decomposed to an amorphous residue upon heating from 90 to 200 °C,<sup>28</sup> there are some noisy patterns with a reduction in the peak size and the definition in the XRD diffractogram of the solid. Hence the shape of the crystal recovered was different from the familiar needle-like structure of struvite. However, the solid recovered had the same surface characteristics of a pure struvite crystal. Both of them had a flake-like structure and triangular cavity on the surface, revealing the same lattice arrangement.<sup>29</sup>

**3.2.4.2. FTIR Analysis.** A broad band was observed at 3452  $\text{cm}^{-1}$  in the FTIR spectrum of struvite precipitate, belonging to the H–O–H stretching vibration of water. The band at 2389  $\text{cm}^{-1}$  was assigned to H–O–H stretching vibration of a cluster of water molecules. The symmetric bending vibration of N–H in  $\text{NH}_4^+$  was at 1689  $\text{cm}^{-1}$ . The band seen at 1474  $\text{cm}^{-1}$  was the asymmetric bending vibration of N–H of  $\text{NH}_4^+$ . The symmetric and asymmetric stretching vibrations of  $\text{PO}_4^{3-}$  units were observed at 910 and 1120  $\text{cm}^{-1}$ , respectively. The band at 574  $\text{cm}^{-1}$  was due to the metal–oxygen bond. The FTIR spectra (Figure 6c) of the struvite precipitate exhibited the characteristic  $\text{PO}_4^{3-}$  band at 1120  $\text{cm}^{-1}$ , the characteristic  $\text{NH}_4^+$  band at 1474  $\text{cm}^{-1}$ , and the band of metal–oxygen at 574  $\text{cm}^{-1}$ , respectively. A similar spectrum for struvite has been reported in the literature.<sup>30</sup>

**3.3. Cost Evaluation on Modified Solvay Process and Struvite Precipitation.** The economic evaluation for the removal of  $\text{Na}^+$  as  $\text{NaHCO}_3$  from 1 L of the textile dye bath

effluent using modified Solvay process and the removal of  $\text{NH}_4^+$  as struvite from 1 L of the supernatant of the process was carried out. In this assessment, only the cost toward the consumption of chemicals and the electrical energy were taken into account. The market prices of the chemicals used and energy consumed for the removal of  $\text{Na}^+$  and the precipitation of struvite are given in Table 1. It could be calculated that the

Table 1. Cost Evaluation of Modified Solvay process and Struvite Precipitation

process	nature of consumable	consumption per liter	price (\$)	total operating cost (\$)
modified Solvay process	ammonia solution	0.144 L	0.086	0.098
	electrical energy	0.15 kWh	0.012	
struvite precipitation	$\text{MgCl}_2 \cdot 6\text{H}_2\text{O}$	0.207 kg	0.180	1.105
	$\text{K}_2\text{HPO}_4$	0.237 kg	0.567	
	NaOH	0.010 kg	0.020	
	electrical energy	4.14 kWh	0.338	

total operating cost of the struvite precipitation was \$1.105/L and for the recovery of  $\text{NaHCO}_3$ , it was \$0.098/L. The recovered  $\text{NaHCO}_3$  and struvite were 0.038 and 0.378 kg, respectively. About 25% of the net operating cost for the modified Solvay process and the struvite precipitation could be reduced by marketing the recovered sodium bicarbonate and the struvite at a favorable price of \$0.023 and \$0.227, respectively.

#### 4. CONCLUSION

This paper was focused on how the briny textile dye bath effluent could be used as a raw material for the valuable bicarbonate chemical production using carbon dioxide gas. From the experimental results, it can be concluded that the highest  $\text{Na}^+$  removal of 38% could be obtained and the optimized reaction conditions were as follows:  $\text{NH}_4\text{OH}/\text{Na}^+$  ratio of 2, reaction temperature of 20 °C, flow rate of the  $\text{CO}_2$  of 1.8 L/min, and carbonation time of 150 min. Among various reaction conditions, 1 M of  $\text{Mg}^{2+}$ , 1.4 M of  $\text{PO}_4^{3-}$ , and solution pH of about 8.5, rendered the best removal efficiency of 80% for  $\text{NH}_4^+$  from the resulting solution of the modified Solvay process. The collected precipitate was positively identified as struvite by XRD, FTIR, and SEM analyses. The results indicate that the new approach can be designed to reduce carbon dioxide gas emissions, as well as to decrease the  $\text{Na}^+$  in textile effluent by recovering it as sodium bicarbonate.

#### AUTHOR INFORMATION

##### Corresponding Author

\*Tel: + 914422359014. Fax: + 914422354717. E-mail: kpvelu@annauniv.edu (K. Palanivelu).

##### Notes

The authors declare no competing financial interest.

#### ACKNOWLEDGMENTS

It is a pleasure for us to thank the UGC-CPEES PHASE II, New Delhi, for the financial support.

#### REFERENCES

- (1) Song, C.; Gaffney, A. F.; Fujimoto, K.  $\text{CO}_2$  conversion and utilization: an overview. *ACS Symp. Ser.* **2002**, 809, 112–116.

- (2) Yoshida, M.; Fujita, M.; Ishii, T.; Ihara, M. A novel methodology for the synthesis of cyclic carbonates based on the palladium - catalyzed cascade reaction of 4-methoxycarbonyloxy-2-butyne-1-ols with phenols, involving a novel carbon dioxide elimination-fixation process. *J. Am. Chem. Soc.* **2003**, *125*, 4874–4881.
- (3) Huijgen, W. J. J.; Comans, R. N. J. Carbon dioxide sequestration by mineral carbonation: Literature review, ECN-C-03-016, 2003.
- (4) Huang, H. P.; Shi, Y.; Li, W.; Chang, S. G. Dual alkali approaches for the capture and separation of CO<sub>2</sub>. *Energy Fuels* **2001**, *15*, 263–268.
- (5) El-Naas, M. H.; Al-Marzouqi, A. H.; Chaalal, O. A combined approach for the management of desalination rejects brine and capture of CO<sub>2</sub>. *Desalination* **2010**, *251*, 70–74.
- (6) Ahmed, M.; Arakel, A.; Hoey, D.; Thumarukudy, M. R.; Goosen, M. F. A.; Al-Haddabi, M.; Al-Belushi, A. Feasibility of salt production from inland RO desalination plant rejects brine: A case study. *Desalination* **2003**, *158*, 109–117.
- (7) Ranganathan, K.; Karunakaran, K.; Sharma, D. C. Recycling of wastewaters of textile dyeing industries using advanced treatment technology and cost analysis - case studies. *Resour., Conserv. Recycl.* **2007**, *50*, 306–318.
- (8) Jeppesen, T.; Shu, L.; Keir, G.; Jegtheesan, V. Metal recovery from reverse osmosis concentrate. *J. Cleaner Prod.* **2009**, *17*, 703–707.
- (9) Boopathy, R.; Gnanamani, A.; Mandal, A. B.; Sekaran, G. A first report on the selective precipitation of sodium chloride from the evaporated residue of reverse osmosis reject salt generated from the leather industry. *Ind. Eng. Chem. Res.* **2012**, *51*, 5527–5534.
- (10) El-Naas, M. H. A different approach for carbon capture and storage (CCS). *Res. J. Chem. Environ.* **2008**, *12*, 3–4.
- (11) Jeffery, G. H.; Bassett, J.; Mendham, J.; Denney, R. C. Vogel's textbook of quantitative chemical analysis, 5th ed.; Longman Scientific and Technical: New York, 1989.
- (12) Eaton, A. D.; Clesceri, L. S.; Rice, E. W.; Greenberg, A. E.; Franson, M. A. H. Standard methods for the examination of water and wastewater, 21st ed.; American Public Health Association: Washington, DC, 2005.
- (13) Jibril, B. E. -Y.; Ibrahim, A. A. Chemical conversions of salt concentrate from desalination plants. *Desalination* **2001**, *139*, 287–295.
- (14) Andel, E. Process for the combined manufacture of chlorinated hydrocarbons and sodium bicarbonate. United States Patent 4,256,719, 1981.
- (15) Dutcher, B.; Fan, M.; Leonard, B. Use of multifunctional nanoporous TiO (OH)<sub>2</sub> for catalytic NaHCO<sub>3</sub> decomposition - eventually for Na<sub>2</sub>CO<sub>3</sub>/NaHCO<sub>3</sub> based CO<sub>2</sub> separation technology. *Sep. Purif. Technol.* **2011**, *80*, 364–374.
- (16) Yang, J. J.; Cheng, H.; Frost, R. L. Synthesis and characterization of cobalt hydroxyl carbonate Co<sub>2</sub>CO<sub>3</sub> (OH)<sub>2</sub> nanomaterials. *Spectrochim. Acta, Part A* **2011**, *78*, 420–428.
- (17) Natale, I. M.; Helmy, A. K. Solid-state reaction of sodium carbonate with montmorillonite at 550°C. *Clays Clay Miner.* **1989**, *37*, 89–95.
- (18) Chowdhury, A.; Bould, J.; Londesborough, M. G. S.; Milne, S. J. The effect of refluxing on the alkoxide-based sodium potassium niobate sol-gel System: thermal and spectroscopic studies. *J. Solid State Chem.* **2011**, *184*, 317–324.
- (19) Chen, X.; Griesser, U. J.; Te, R. L.; Pfeiffer, R. R.; Morris, K. R.; Stowell, J. G.; Byrn, S. R. Analysis of the acid-base reaction between solid indomethacin and sodium bicarbonate using infrared spectroscopy, X-ray powder diffraction, and solid-state nuclear magnetic resonance spectroscopy. *J. Pharm. Biomed.* **2005**, *38*, 670–677.
- (20) Etter, B.; Tilley, E.; Khadka, R.; Udert, K. M. Low-cost struvite production using source-separated urine in Nepal. *Water Res.* **2011**, *45*, 852–862.
- (21) Korchef, A.; Saidou, H.; Amor, M. B. Phosphate recovery through struvite precipitation by CO<sub>2</sub> removal: Effect of magnesium, phosphate and ammonium concentrations. *J. Hazard. Mater.* **2011**, *186*, 602–613.
- (22) Mijangos, F.; Kamel, M.; Lesmes, G.; Muraviev, D. N. Synthesis of struvite by ion exchange isothermal super saturation technique. *React. Funct. Polym.* **2004**, *60*, 151–161.
- (23) Ronteltap, M.; Maurer, M.; Hausherr, R.; Gujer, W. Struvite precipitation from urine—influencing factors on particle size. *Water Res.* **2010**, *44*, 2038–2046.
- (24) Stratful, I.; Scrimshaw, M. D.; Lester, J. N. Conditions influencing the precipitation of magnesium ammonium phosphate. *Water Res.* **2001**, *35*, 4191–4199.
- (25) Huang, H.; Xu, C.; Zhang, W. Removal of nutrients from piggery wastewater using struvite precipitation and pyrogenation technology. *Bioresour. Technol.* **2011**, *102*, 2523–2528.
- (26) Maekawa, T.; Liao, C. M.; Feng, X. D. Nitrogen and phosphorus removal for swine wastewater using intermittent aeration batch reactor followed by an ammonium crystallization process. *Water Res.* **1995**, *29*, 2643–2650.
- (27) Ryu, H. D.; Lim, C. S.; Kang, M. K.; Lee, S. I. Evaluation of struvite obtained from semiconductor wastewater as a fertilizer in cultivating Chinese cabbage. *J. Hazard. Mater.* **2012**, *221–222*, 248–255.
- (28) Kurtulus, G.; Tas, A. C. Transformations of neat and heated struvite (MgNH<sub>4</sub>PO<sub>4</sub> 6H<sub>2</sub>O). *Mater. Lett.* **2011**, *65*, 2883–2886.
- (29) Babic-Ivancic, V.; Kontrec, J.; Kralj, D.; Brecevic, L. Precipitation diagrams of struvite and dissolution kinetics of different struvite morphology. *Croat. Chem. Acta.* **2002**, *75*, 89–106.
- (30) Chauhan, C. K.; Joshi, M. J. In vitro crystallization, characterization, and growth- inhibition study of urinary type struvite crystals. *J. Cryst. Growth.* **2013**, *362*, 330–337.